ELSEVIER

Thermochimica Acta 245 (1994) 219-229

thermochimica
acta

Re-entrant behaviour in pressure-composition phase diagrams of liquid crystals ☆

A. Daoudi [a,]*, A. Anakkar [b], J.-M. Buisine [a]

[a] *Laboratoire de Dynamique et Structure des Matériaux Moléculaires, U.R.A. CNRS no. 801, Equipe de Thermophysique de la Matière Condensée, Université du Littoral-Quai Freycinet 1, B.P. 5526, F-59379 Dunkerque, France*

[b] *Laboratoire de Dynamique et Structure des Matériaux Moléculaires, U.R.A. CNRS no. 801, Equipe de Physique des Stases Anisotropes, Université des Sciences et Technologies de Lille, F-59666 Villeneuve d'Ascq Cédex, France*

Abstract

For liquid crystalline pure compounds exhibiting re-entrant phenomena the chemical potential difference between two successive phases along the isotherm is supposed to have simple pressure dependence. For binary mixtures of such compounds the thermodynamic approach called equal Gibbs energy analysis is applied to the study of their pressure-composition phase diagrams. Many types of isothermal phase diagrams which exhibit re-entrant phase behaviour can be predicted by assuming perfect or non-perfect nature (regular and non-zero excess molar volume) of the solutions. For the mesogenic system hexyloxy-octyloxy cyanobiphenyl, it is shown that the pressure-composition phase diagram is more successfully described with a regular solution hypothesis than with a perfect hypothesis.

Keywords: Composition; Liquid crystal; Pressure; Re-entrant

---

1. Introduction

For liquid crystals, mesophases are usually obtained from pure organic compounds (mesogens) with rod-like molecular structure which consist of a rigid

---

☆ Presented at the Czechoslovak-French-Polish Conference on Calorimetry and Experimental Thermodynamics: Applications to Contemporary Problems, Prague, Czech Republic, 4-7 September 1993.

* Corresponding author.

SSDI 0040-6031(94)01842-5

central core (mainly benzenic rings) extended by flexible parts such as aliphatic chains. Two main classes of this intermediate phase are the orientationally ordered nematic (N) phase with no long-range correlation between the mass centres of the molecules, and the layered phases (usually called smectic phases (S)) of which the common feature is the arrangement of the molecular centres in equidistant planes. We can distinguish mainly the smectic A (S_A) and smectic C (S_C) phases where the molecular orientation is, respectively, perpendicular to the layers and tilted with respect to the layer normal.

Usually, in phase transitions, the higher temperature phase is globally less ordered (more symmetric) than the lower temperature phase. This behaviour leads, for rod-like mesogens, to normal sequences such as KSNI where the symbols K and I denote crystalline and isotropic liquid phases. However, it is not a law of thermodynamics that symmetry and global order go hand in hand and, sometimes, a more symmetric phase reappears at a lower temperature than the less symmetric one, which leads to re-entrant sequences. Of the re-entrant mesophases the most common are the nematic, smectic A and smectic C phases [1] which have generally been exhibited by rod-like mesogens whose molecules possess a strongly polar end group [2].

A considerable amount of experimental work has been carried out for these mesogenic systems, in order to study the effect of thermodynamic parameters such as pressure, temperature and composition on re-entrant phenomena in their phase diagrams. Some efforts to give thermodynamic descriptions of such diagrams have been reported using macroscopic approaches for calculating both pressure-temperature phase diagrams for pure compounds and binary isobaric phase diagrams exhibiting one [3-5] and two [6,7] re-entrant mesophases. A variety of isobaric phase diagrams of binary mixtures exhibiting double re-entrances have also been treated by means of a microscopic approach [8], where many types of observed phase diagrams were described and new topologies were predicted.

However, to our knowledge, for binary mesogenic mixtures no systematic studies have been undertaken to describe re-entrant phenomena in isothermal pressure-composition phase diagrams. It is the purpose of this paper to present a theoretical study in order to predict the $P-x$ curves of polar liquid crystalline mixtures exhibiting re-entrant behaviour. For calculating the pressure-composition equilibrium curves, the equal G analysis [9], which consists of setting equal the total Gibbs energies of two phases in equilibrium, seems to be suitable because of the missing or the narrowness of the biphasic regions in phase diagrams for re-entrant systems [5,10]. This also considerably reduces the calculations. The mesomorphous solution hypothesis, which has already been used successfully [11], is retained in this study. Furthermore, re-entrant phase diagrams will be described thermodynamically in terms of ideal and non-ideal solutions.

2. Equal *G* equation

The general form of the total Gibbs energy for any phase of binary mixtures at pressure P and temperature T is

$$G(T,P,x) = (1-x)\mu_1(T,P,x) + x\mu_2(T,P,x) \tag{1}$$

in which x is taken to be the mole fraction of component 2, and μ_1 and μ_2 are, respectively, the chemical potentials of components 1 and 2 in the phase of interest. Taking into account the usual expression for the chemical potential of component i

$$\mu_i(T,P,x) = \mu_1^*(T,P) + RT\ln(xi) + \mu_i^{\mathrm{E}} \tag{2}$$

the total Gibbs energy can be written as

$$G(T,P,x) = (1-x)\mu_1^* + x\mu_2^* + RT[(10x)\ln(1-x) + x\ln x] + G^{\mathrm{E}} \tag{3}$$

where μ_1^* and μ_2^* are the chemical potentials of pure components. The logarithmic term is the ideal Gibbs energy of mixing and the term G^{E} is the excess Gibbs energy. Consider now, for a binary system, two phases α and β the compositions of which are respectively x^α and x^β. The equilibrium between α and β, at given pressure and temperature, is defined by the criteria that the chemical potentials of each component in each phase are equal. However, for rod-like mesogens exhibiting re-entrant phenomena, since the enthalpy and volume changes associated with the transformations between the phases are very low (50 J mol^{-1} and 0.01 cm^3 mol^{-1} respectively) [12,13], the equal G analysis can be used to describe the binary phase diagrams and hence leads to a good description of the equilibrium curves. Thus, by setting equal the total Gibbs energy (Eq. 3) for α and β phases, the equal G equation is given by

$$(1-x)\Delta\mu_1^{*\alpha\beta}(T,P) + x\Delta\mu_2^{*\alpha\beta} + \Delta G^{\mathrm{E}\alpha\beta}(T,P,x) = 0 \tag{4}$$

This relation gives the isothermal or isobaric phase diagram consisting of the phase boundary line describing the equilibrium between α and β phases. In order to calculate the isothermal pressure–composition curves, expressions for $\Delta\mu_1^{*\alpha\beta}$ and $\Delta G^{\mathrm{E}\alpha\beta}$, at a given temperature, are required.

3. Chemical potential expressions of pure components

Consider at first the chemical potential μ_i^* of pure component i. Since

$$\left(\frac{\partial\mu_i^*}{\partial P}\right)_T = V_i^* \tag{5}$$

and

$$\left(\frac{\partial^2\mu_i^*}{\partial P^2}\right)_T = \left(\frac{\partial V_i^*}{\partial P}\right)_T = -\chi_i V_i^* \tag{6}$$

Then

$$\mu_i^*(P) - \mu_i^*(P_i^{\alpha\beta}) = V_i^*(P_i^{\alpha\beta})[P - P_i^{\alpha\beta}] - \int_{P_i^{\alpha\beta}}^{P}\left(\int_{P_i^{\alpha\beta}}^{P}\chi_i V_i^*\,\mathrm{d}P\right)\mathrm{d}P \tag{7}$$

where $P_i^{\alpha\beta}$ is an α–β transition pressure at temperature T, and V_i^* and χ_i are respectively molar volume and compressibility of pure component i. The difference between the chemical potentials of two phases α and β as a function of pressure is then given by

$$\begin{aligned}\Delta\mu_i^{*\alpha\beta}(P) &= \mu_i^{*\beta}(P) - \mu_i^{*\alpha}(P)\\ &= \Delta V_i^{*\alpha\beta}(P_i^{\alpha\beta})[P - P_i^{\alpha\beta}] - \int_{P_i^{\alpha\beta}}^{P}\left(\int_{P_i^{\alpha\beta}}^{P}(\chi_i^{\beta}V_i^{*\beta} - \chi_i^{\alpha}V_i^{*\alpha})\,\mathrm{d}P\right)\mathrm{d}P \qquad (8)\end{aligned}$$

where $\Delta V_i^{*\alpha\beta}$ is the molar volume change at the transition pressure $P_i^{\alpha\beta}$ and noting here that β is considered to be the lower pressure phase. The equilibrium between α and β will occur for each pressure P when the condition $\Delta\mu_i^{*\alpha\beta}(P) = 0$ is satisfied. If only one possibility of a phase transition between α and β phases exists (normal sequence), the effect of compressibility (which is described by the integral in Eq. (8)) can be neglected. However the expression for $\Delta\mu_i^{*\alpha\beta}(P)$ must include the compressibility term in order to take into account the reappearance, for pure component i, of the β phase at higher pressure. This in fact requires that the slopes of the chemical potentials versus pressure of α and β phases must be sufficiently different to ensure re-entrant behaviour; in other words the chemical potential curves of the two phases must cross twice at the two transition pressure $P_{iB}^{\alpha\beta}$ and $P_{iH}^{\alpha\beta}$ (Fig. 1(a)). For a pure component i to exhibit the re-entrant sequence $\beta-\alpha-\beta_{re}$ at isotherm T (Fig. 1(b)) we suppose in the first approximation a linear dependence on pressure of molar volume for each phase following these two relations

$$V_i^{*\alpha}(P) = a^{\alpha}P + b^{\alpha} \qquad (9a)$$

$$V_i^{*\beta}(P) = a^{\beta}P + b^{\beta} \qquad (9b)$$

Using Eq. (6) and carrying out the integration in Eq. (8) we obtain

$$\Delta\mu_i^{*\alpha\beta}(P) = \Delta V_i^{*\alpha\beta}(P_{iB}^{\alpha\beta})[P - P_{iB}^{\alpha\beta}] + \frac{c^{\alpha\beta}}{2}[P - P_{iB}^{\alpha\beta}]^2$$

where $c^{\alpha\beta} = a^{\beta} - a^{\alpha}$ and $P_i^{\alpha\beta}$ of Eq. (8) has been called $P_{iB}^{\alpha\beta}$, the lower phase transition pressure. The phase equilibrium condition $\Delta\mu_i^{*\alpha\beta}(P_{iH}^{\alpha\beta}) = 0$ between α and

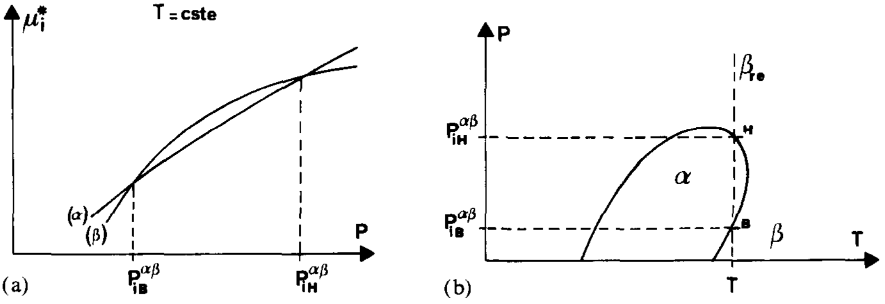

Fig. 1. (a) Chemical potential curves at temperature T of α and β phases versus pressure for a component exhibiting a $\beta-\alpha-\beta_{re}$ sequence. (b) Typical pressure–temperature phase diagram for a pure component which at temperature T exhibits the sequence $\beta-\alpha-\beta_{re}$.

β at the higher transition $P_{i\mathrm{H}}^{\alpha\beta}$ allows $c^{\alpha\beta}$ to be determined and the expression of chemical potential difference can be deduced

$$\Delta\mu_i^{*\alpha\beta}(P) = \Delta V_i^{*\alpha\beta}(P_{i\mathrm{B}}^{\alpha\beta})\,\frac{(P - P_{i\mathrm{B}}^{\alpha\beta})(P_{i\mathrm{H}}^{\alpha\beta} - P)}{(P_{i\mathrm{H}}^{\alpha\beta} - P_{i\mathrm{B}}^{\alpha\beta})} \tag{10}$$

4. Isothermal phase diagrams for re-entrant binary mixtures

To predict isothermal pressure–composition phase diagrams for re-entrant binary mixtures, two hypotheses are considered according to the nature of solutions: (i) the perfect solution hypothesis; (ii) the non-perfect solution hypothesis.

4.1. Perfect solution hypothesis

With the perfect solution hypothesis, setting the excess Gibbs energies equal to zero in Eq. (4) gives

$$(1 - x)\Delta\mu_1^{*\alpha\beta} + x\Delta\mu_2^{*\alpha\beta} = 0 \tag{11}$$

In this case one should distinguish two situations. Either only one component in the mixture exhibits re-entrant behaviour, or both pure components of mixture show the same re-entrant sequence at a given temperature.

In the first situation, for the non-re-entrant component, which we shall call component 2, we suppose that the β phase is more stable than the α phase in the pressure range between the transition pressures $P_{i\mathrm{H}}^{\alpha\beta}$ and $P_{i\mathrm{B}}^{\alpha\beta}$ of the re-entrant component (component 1). The component 2 can, however, exhibit a real or virtual [11] α phase. Assuming that there is no possibility of transition from the β to the α phase for component 2, the following form of $\Delta\mu_2^{*\alpha\beta}$ can be used:

$$\Delta\mu_2^{*\alpha\beta} = \Delta V_2^{*\alpha\beta}(P - P_2^{\alpha\beta}) \tag{12}$$

where $P_2^{\alpha\beta}$ and $\Delta V_2^{*\alpha\beta}$ are the pressure and the molar volume change at real or virtual transition of component 2. Eq. (11) can be solved, after replacing $\Delta\mu_1^{*\alpha\beta}$ and $\Delta\mu_2^{*\alpha\beta}$ by Eqs. (10) and (12), respectively to give the expression of composition as a function of pressure

$$x = \frac{\Delta V_1^{*\alpha\beta}(P - P_{1\mathrm{B}}^{\alpha\beta})(P_{1\mathrm{H}}^{\alpha\beta} - P)}{\Delta V_1^{*\alpha\beta}(P - P_{1\mathrm{B}}^{\alpha\beta})(P_{1\mathrm{H}}^{\alpha\beta} - P) - \Delta V_2^{*\alpha\beta}(P - P_2)(P_{1\mathrm{H}}^{\alpha\beta} - P_{1\mathrm{B}}^{\alpha\beta})} \tag{13}$$

Eq. (13) allows the equilibrium curve in the isothermal pressure–composition phase diagram to be described when only one of the two mixing components exhibits re-entrant behaviour. The general form of the isothermal phase diagram likely to be experimentally observed in this case is shown in Fig. 2. It can be noted that the equilibrium curve of the two phases α and β is situated entirely between the two transition pressures of the re-entrant component.

In the second situation, where both components of the mixture exhibit the same re-entrant sequence the expressions of the chemical potential differences of compo-

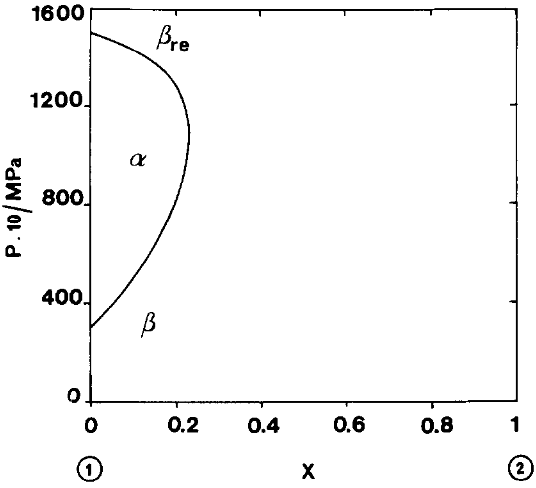

Fig. 2. The calculated isothermal pressure–composition phase diagram obtained using the perfect solution hypothesis when only component 1 exhibits a re-entrant sequence.

nents 1 and 2 are given by Eq. (10). After substituting Eq. (10) into Eq. (11), the equal G equation (Eq. (11)) can then be solved for composition as a function of pressure.

$$x = \frac{\Delta V_1^{*\alpha\beta}(P - P_{1B}^{\alpha\beta})(P_{1H}^{\alpha\beta} - P)(P_{2H}^{\alpha\beta} - P_{2B}^{\alpha\beta})}{\Delta V_1^{*\alpha\beta}(P - P_{1B}^{\alpha\beta})(P_{1H}^{\alpha\beta} - P)(P_{2H}^{\alpha\beta} - P_{2B}^{\alpha\beta}) - \Delta V_2^{*\alpha\beta}(P - P_{2B}^{\alpha\beta})(P_{2H}^{\alpha\beta} - P)(P_{1H}^{\alpha\beta} - P_{1B}^{\alpha\beta})} \tag{14}$$

This equation allows calculation of the equilibrium curve between α and β phases in the pressure–composition phase diagram, when all characteristic quantities of pure components are known. Two types of isothermal phase diagrams for binary mixtures of re-entrant mesogens have been calculated using Eq. (14) and are presented in Fig. 3. If $P_{1B}^{\alpha\beta} < P_{2B}^{\alpha\beta} < P_{1H}^{\alpha\beta}$, one α phase domain is obtained (Fig. 3(a)) and the $\beta-\alpha-\beta_{re}$ sequence exists for all compositions. If, on the contrary, $P_{2B}^{\alpha\beta} > P_{1H}^{\alpha\beta}$, two disjointed α phase domains are obtained (Fig. 3(b)) and then the $\beta-\alpha-\beta_{re}$ sequence exists only for two finite composition ranges.

4.2. Non-perfect solution hypothesis

Here only the case where one component exhibits a re-entrant sequence is considered. For non-perfect solutions, the equal G equation (Eq. (4)) becomes in this case

$$(1-x)\left[\Delta V_1^{*\alpha\beta}\frac{(P - P_{1B}^{\alpha\beta})(P_{1H}^{\alpha\beta} - P)}{(P_{1H}^{\alpha\beta} - P_{1B}^{\alpha\beta})}\right] + x\Delta V_2^{*\alpha\beta}(P - P_2) + \Delta G^{E\alpha\beta} = 0 \tag{15}$$

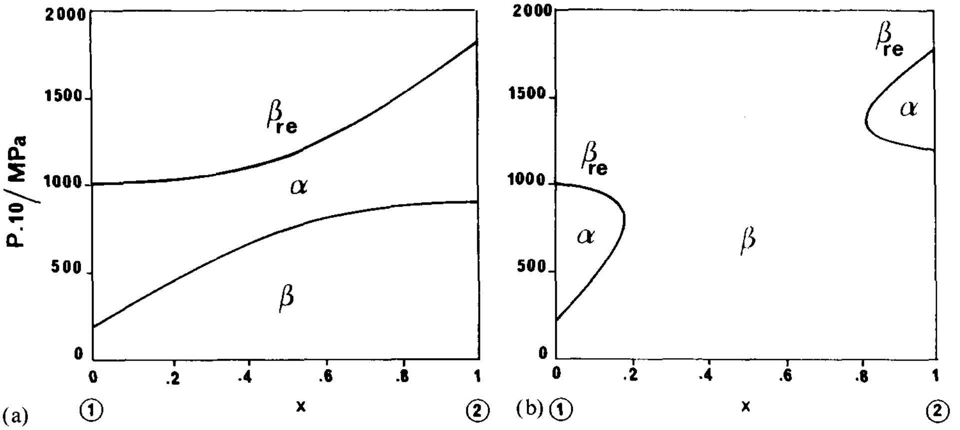

Fig. 3. The calculated isothermal pressure–composition phase diagrams obtained using the perfect solution hypothesis when both components of the mixture exhibit the sequence β–α–β_{re}: (a) $P_{1B}^{\alpha\beta} < P_{2B}^{\alpha\beta} < P_{1H}^{\alpha\beta}$; (b) $P_{2B}^{\alpha\beta} > P_{1H}^{\alpha\beta}$.

where the excess Gibbs energy term $\Delta G^{E\alpha\beta}$ shows the non-perfect nature of solutions and is generally dependent on pressure, temperature and composition. Several mathematical forms can be used as an expression for G^E; that most usually used is the Redlich–Kister expression [9]

$$G^E = x(1-x)\sum_j A_j(1-2x)^{1-j} \tag{16}$$

Taking into account only the first term in the expansion, the most simple form

$$G^E = Ax(1-x) \tag{17}$$

can be used for the excess Gibbs energy where A is the interaction parameter describing the intermolecular forces between the components of mixtures. In order to study the influence of the excess quantities upon the topology of isothermal phase diagrams for re-entrant systems two types of non-perfect solution have been considered: (1) regular solutions which require no dependence of G^E on pressure and temperature [14]; (2) non-zero excess molar volume solutions assuming a simple dependence of the excess Gibbs energy on pressure.

4.2.1. Regular solutions

In regular solution theory, the expression of the excess Gibbs energy for a binary mixture in phase α is written as

$$G^{E\alpha} = A^\alpha x(1-x) \tag{18}$$

where the parameter A^α is independent of pressure and temperature. Thus, the excess Gibbs energy difference between two phases α and β is given by

$$\Delta G^{E\alpha\beta} = (A^\beta - A^\alpha)x(1-x) \tag{19}$$

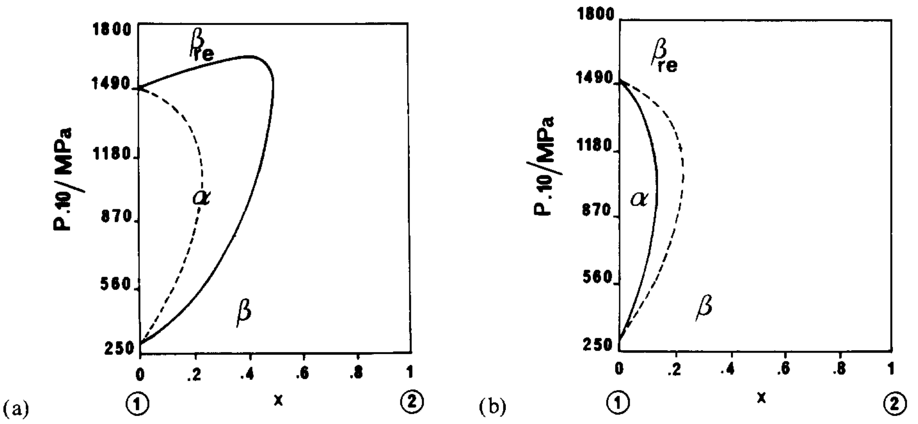

Fig. 4. The calculated isothermal pressure–composition phase diagrams obtained using the regular solution hypothesis (solid line) when only component 1 exhibits a re-entrant sequence: (a) $A^\beta - A^\alpha > 0$; (b) $A^\beta - A^\alpha < 0$. Broken lines are the calculated equilibrium curves obtained using the perfect solution hypothesis.

Replacing Eq. (19) in the equal G equation (Eq. (15)) leads to the relation (20) that describes the equilibrium curves in pressure–composition phase diagrams when only one of the mixing components is re-entrant.

$$\begin{aligned}&(1-x)\Delta V_1^{*\alpha\beta}P^2[(1-x)\Delta V_1^{*\alpha\beta}(P_{1H}^{\alpha\beta}+P_{1B}^{\alpha\beta})+x\Delta V_2^{*\alpha\beta}(P_{1H}^{\alpha\beta}-P_{1B}^{\alpha\beta})]P\\&+(1-x)\Delta V_1^{*\alpha\beta}P_{1H}^{\alpha\beta}P_{1B}^{\alpha\beta}+x\Delta V_2^{*\alpha\beta}(P_{1H}^{\alpha\beta}-P_{1B}^{\alpha\beta})P_2\\&-(A^\beta-A^\alpha)(P_{1H}^{\alpha\beta}-P_{1B}^{\alpha\beta})x(1-x)=0\end{aligned}\qquad(20)$$

Using Eq. (20), two possible shapes of isothermal phase diagrams have been obtained according to the sign of the quantity $(A^\beta - A^\alpha)$; they are illustrated in Fig. 4. For comparison, in each part of Fig. 4 the equilibrium curves (dashed lines) calculated by using the perfect solution approximation are shown. For $A^\beta - A^\alpha > 0$ (Fig. 4(a)) the α phase domain tends to increase inducing a decrease of the β phase domain and this is compared to the phase diagram obtained using the perfect solution hypothesis. Note that Eq. (20) can predict the isothermal phase diagrams exhibiting not only re-entrant behaviour but also a maximum (at $P \approx 164.6$ MPa and $x = 0.41$ in Fig. 4(a)). On the contrary for $A^\beta - A^\alpha < 0$, the β phase domain calculated using the regular solution hypothesis is more important than that calculated using the perfect solution hypothesis (Fig. 4(b)). This suggests that, when the mixed mesogens form regular solutions, the mixture favours the phase which has the smaller A parameter, i.e. the phase that exhibits the greater molecular affinity between the components.

4.2.2. Non-zero excess molar volume solutions

For the solutions exhibiting an excess molar volume due to the non-ideality of the mixed components, the excess Gibbs energy (Eq. (17)) is a function of pressure.

Thus, the excess molar volume is given by

$$\left(\frac{\partial G^{\mathrm{E}}}{\partial P}\right)_T = V^{\mathrm{E}} \tag{21}$$

Assuming V^{E} to be constant, the following expression of the excess Gibbs energy can easily be found:

$$G^{\mathrm{E}}(P,x) = (A_0 + Pv^{\mathrm{E}})x(1-x) \tag{22}$$

where A_0 is the $A(P)$ parameter value at atmospheric pressure ($P = 0$) and $v^{\mathrm{E}} = \partial A(P)/\partial P$. Thus the expression for $\Delta G^{\mathrm{E}\alpha\beta}$ is

$$\Delta G^{\mathrm{E}\alpha\beta} = G^{\mathrm{E}\beta} - G^{\mathrm{E}\alpha} = (\Delta A_0^{\alpha\beta} + \Delta v^{\mathrm{E}\alpha\beta}P)x(1-x) \tag{23}$$

Using Eqs. (15) and (23) the relation (24) describing the equilibrium between α and β phases in the pressure–composition phase diagram can be derived:

$$\begin{aligned}
&[(1-x)\Delta V_1^{*\alpha\beta}(P_{1\mathrm{H}}^{\alpha\beta} + P_{1\mathrm{B}}^{\alpha\beta}) + x\Delta V_2^{*\alpha\beta}(P_{1\mathrm{H}}^{\alpha\beta} - P_{1\mathrm{B}}^{\alpha\beta})\\
&\quad + \Delta v^{\mathrm{E}\alpha\beta}(P_{1\mathrm{H}}^{\alpha\beta} - P_{1\mathrm{B}}^{\alpha\beta})x(1-x)]P + (1-x)\Delta V_1^{*\alpha\beta}P_{1\mathrm{H}}^{\alpha\beta}P_{1\mathrm{B}}^{\alpha\beta}\\
&\quad + x\Delta V_2^{*\alpha\beta}(P_{1\mathrm{H}}^{\alpha\beta} - P_{1\mathrm{B}}^{\alpha\beta})P_2 - (A^{\beta} - A^{\alpha})(P_{1\mathrm{H}}^{\alpha\beta} - P_{1\mathrm{B}}^{\alpha\beta})x(1-x) = 0
\end{aligned} \tag{24}$$

Fig. 5 shows an example of the isothermal phase diagrams calculated using Eq. (24) for binary mixtures exhibiting excess molar volumes. Two different diagrams can be obtained according to the sign of the quantity $\Delta A_0^{\alpha\beta}$. The phase diagram presented in Fig. 5(a) well illustrates the influence of the additive energetic term in the expression for $\Delta G^{\mathrm{E}\alpha\beta}$ (Eq. (23)) due to excess molar volumes; the α phase is obtained for all compositions for which $\Delta A_0^{\alpha\beta}$ is positive and the β–α–β_{re} sequence is then observed for almost all mixtures. However when $\Delta A_0^{\alpha\beta}$ is negative (Fig. 5(b)) the β–α–β_{re} sequence is obtained only for mixtures rich (more than 80 mol%) in re-entrant component.

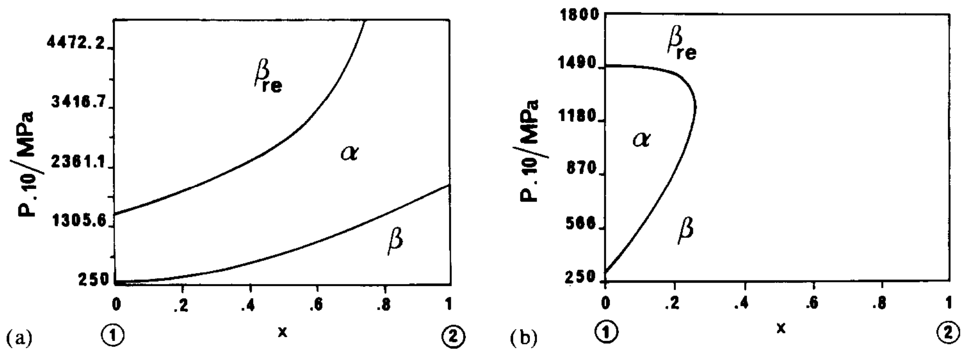

Fig. 5. The calculated isothermal pressure–composition phase diagrams obtained using the non-zero excess molar volume solution hypothesis when only component 1 exhibits a re-entrant sequence: (a) $\Delta A_0^{\alpha\beta} > 0$; (b) $\Delta A_0^{\alpha\beta} < 0$.

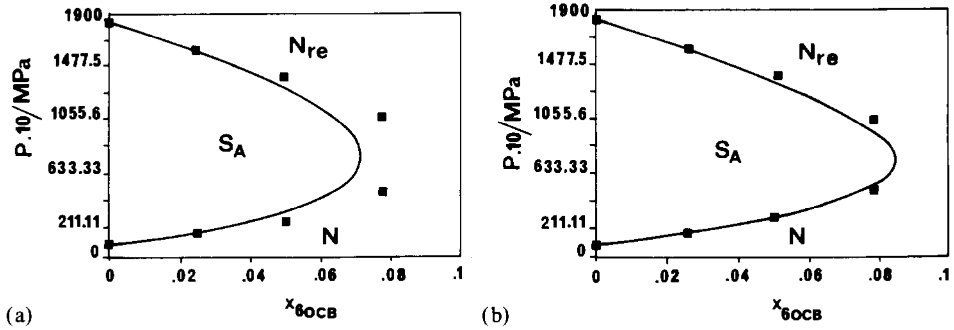

Fig. 6. The calculated isothermal phase diagrams (solid lines) for the re-entrant system 8 OCB + 6 OCB (see text) at $T = 340.5$ K: (a) perfect solution hypothesis; (b) regular solution hypothesis. ■, Experimental points (from Ref. [15]).

5. Application

One experimental example has been found to illustrate this theoretical study. It concerns isothermal phase diagrams extracted from pressure–temperature diagrams of the re-entrant mesogenic system hexyloxycyanobiphenyl (6 OCB) and octyloxycyanobiphenyl (8 OCB) showing the sequence N–S_A–N_{re} [15]. We have compared the calculated perfect and regular solution phase diagrams with the experimental phase diagram determined at $T = 340.5$ K. With the perfect solution hypothesis, $\Delta V_2^{*S_A N}$ and P_2 parameters in Eq. (13) are found using the experimental data for $x_{6OCB} = 0.025$, while in the regular solution hypothesis, the $\Delta V_2^{*S_A N}$, P_2 and $(A^N - A^{S_A})$ parameters in Eq. (20) are determined using experimental data for $x_{6OCB} = 0.025$ and $x_{6OCB} = 0.078$. In Fig. 6 the calculated isothermal phase diagrams and the experimental points are presented. The measured values are more successfully described by the regular solution hypothesis (Fig. 6(b)) than by the perfect solution hypothesis (Fig. 6(a)).

6. Conclusions

For binary mixtures of polar mesogens exhibiting re-entrant behaviour, several types of isothermal phase diagram have been predicted. The equilibrium curves in the pressure–composition diagram have been described in the framework of three different solution models: perfect, regular and non-zero excess molar volume solutions. Comparison between experimental and calculated data for the hexyloxy–octyloxycyanobiphenyl system gives evidence that the pressure–composition phase diagram is successfully described by the regular solution hypothesis.

References

[1] J.-M. Buisine, Thermodyn. Continuum Mech., in press.
[2] H.T. Nguyen, J. Chim. Phys. Phys.-Chim. Biol., 80 (1983) 83.
[3] D.D. Klug and E. Whalley, J. Chem. Phys., 71 (1979) 1874.
[4] N.A. Clark, J. Phys. C3, 40 (1979) 345.
[5] G.R. Van Hecke, J. Phys. Chem., 89 (1985) 2058.
[6] J. Billard, Proc. Int. Liquid Crystals Conf., Bangalore, Heyden, London, 1980, p. 155.
[7] A. Anakkar, Thesis, Lille I, 1990.
[8] J.F. Marko, J.O. Indeken and A.N. Berker, Phys. Rev. A, 39 (1989) 4201.
[9] H.A.J. Oonk, Phase Theory, Elsevier, New York, 1981, p. 71.
[10] G. Illian, H. Kneppe and F. Schneider, Liq. Cryst., 4 (1989) 643.
[11] M. Domon and J. Billard, Pramàna, Suppl. number 1 (1975) 131.
[12] H.T. Nguyen, H. Gasparoux and C. Destrade, Mol. Cryst. Liq. Cryst., 123 (1985) 271.
[13] A. Beguin, J. Billard, F. Bonamy, J.-M. Buisine, P. Cuvelier, J.C. Dubois and P. Le Barny, Mol. Cryst. Liq. Cryst., 131 (1985) 257.
[14] J. Hildebrand and R.L. Scott, Solubility of Non-Electrolytes, 3rd edn., Reinhold, New York, 1950.
[15] P.E. Cladis, D. Guillon, F.R. Bouchet and P.L. Finn, Phys. Rev. A, 23 (1981) 2594.